Published in final edited form as:
Nat Neurosci. 2008 February ; 11(2): 143–151. doi:10.1038/nn2025.

CNS-derived glia ensheath peripheral nerves and mediate motor root development

Sarah Kucenas[1], **Norio Takada**[1], **Hae-Chul Park**[2], **Elvin Woodruff**[1], **Kendal Broadie**[1], and **Bruce Appel**[1]

1*Department of Biological Sciences, Vanderbilt Kennedy Center for Research on Human Development, Vanderbilt Program in Developmental Biology and the Vanderbilt Center for Molecular Neuroscience, Vanderbilt University, Nashville, Tennessee 37235, USA.*

2*School of Medicine, Korea University, Ansan, Gyeonggido 425-707, Republic of Korea.*

Abstract

Motor function requires that motor axons extend from the spinal cord at regular intervals and that they are myelinated by Schwann cells. Little attention has been given to another cellular structure, the perineurium, which ensheaths the motor nerve, forming a flexible, protective barrier. Consequently, the origin of perineurial cells and their roles in motor nerve formation are poorly understood. Using time-lapse imaging in zebrafish, we show that perineurial cells are born in the CNS, arising as ventral spinal-cord glia before migrating into the periphery. In embryos lacking perineurial glia, motor neurons inappropriately migrated outside of the spinal cord and had aberrant axonal projections, indicating that perineurial glia carry out barrier and guidance functions at motor axon exit points. Additionally, reciprocal signaling between perineurial glia and Schwann cells was necessary for motor nerve ensheathment by both cell types. These insights reveal a new class of CNS-born glia that critically contributes to motor nerve development.

The formation of spinal motor nerves requires coordinated interactions between several types of cells. Motor neurons extend axons into developing muscle fields from the spinal cord through segmentally positioned motor exit points (MEPs). These axons encounter neural crest–derived boundary cap cells clustered at MEPs, which permit the axons, but not the cell bodies, to exit from the spinal cord[1]. As motor axons approach their targets, they are sequentially wrapped and then myelinated by Schwann cells, glial cells that also develop from neural crest.

The myelinated motor nerve is surrounded by a flexible cellular sheath called the perineurium, first described in 1841 by Henle and later named by Key and Retzius[2]. The perineurium consists of uninterrupted, concentric rings of flattened cells that are connected by tight junctions and encase motor nerves from the MEP to the neuromuscular junction (NMJ)[2–7]. The perineurial sheath serves as a barrier, protecting axons from ionic flux, toxins and infection[4, 8–10]. Therefore, formation of the perineurium is essential for peripheral nerve function.

Correspondence should be addressed to B.A. (b.appel@vanderbilt.edu).

AUTHOR CONTRIBUTIONS

S.K. produced all of the data except for the electron microscopy images shown in Figure 5c,d, which were produced by E.W. N.T. created the *Tg(sox10(7.2):mrfp)* transgenic line and H.-C.P. created the *Tg(olig2:dsred2)* transgenic line. B.A. supervised the experiments and wrote the manuscript with S.K. and K.B.

Published online at http://www.nature.com/natureneuroscience

Previous studies have suggested that, during development, the perineurium appears to form by a series of steps in which nearby mesenchymal cells first assemble as a loosely organized tube around the nerve and then mature to create a multilayered barrier[11]. The maturation step requires the signaling molecule Desert hedgehog (Dhh), which is expressed by Schwann cells. In the absence of Dhh, the perineurium is disorganized and is permeable to macromolecules and inflammatory cells[12]. Although these studies revealed a critical feature of perineurial cell differentiation, the origin of perineurial cells and how they initially associate with motor nerves remain unknown.

In *Drosophila*, motor axon–ensheathing glia are born in the lateral edges of the CNS and then migrate out in a chain-like fashion along the motor nerve[13–17]. The peripheral ensheathing glia of flies and peri-neurial cells of vertebrates have similar functional properties, raising the possibility that they have similar developmental origins. We tested this hypothesis by investigating the origin and development of perineurial cells in zebrafish. Using transgenic reporter genes and time-lapse imaging, we directly determined that, as in *Drosophila*, glial cells born in the CNS migrate into the periphery to ensheath motor nerves. Specifically, we observed that ventral spinal-cord glia emerged from MEPs and migrated along the entire length of motor axons, ensheathing both axons and Schwann cells and forming the perineurium. In the absence of these perineurial cells, we saw that motor axons exited the spinal cord ectopically and Schwann cells failed to wrap motor nerves, indicating that these cells help direct development of spinal ventral nerve roots. Finally, we observed that perineurial glia failed to ensheath motor nerves in mutant embryos with defective Schwann cell development, suggesting that the wrapping behavior of perineurial glia is instructed by signals derived from Schwann cells. These studies reveal intimate, orchestrated interactions between motor neurons, Schwann cells and perineurial glia in the formation of peripheral motor nerves.

RESULTS

nkx2.2a$^+$ cells ensheath motor axons and Schwann cells

In *Drosophila*, glial cells that wrap motor nerves originate in the CNS, close to motor neurons[13,16]. In zebrafish, lateral floor plate cells are immediately ventral to motor neurons[18] and, consequently, in a position to similarly interact with pathfinding motor axons. We therefore hypothesized that zebrafish perineurial cells arise from the lateral floor plate. To test this idea, we used *in situ* RNA hybridization to examine the expression of genes that have been previously associated with the lateral floor plate. Ventral spinal-cord cells expressed *nkx2.2a, nkx2.2b, foxa (fkd4), foxa2 (fkd1), nkx6.2* and *nkx2.9* (data not shown). Among these markers, only *nkx2.2a* was expressed outside the CNS in a pattern that is consistent with the distribution of ventral motor nerves.

We investigated *nkx2.2a* expression in detail by observing the distribution of *nkx2.2a* RNA and enhanced green fluorescent protein (EGFP) encoded by a transgene (Fig. 1). At 24 and 36 h postfertilization (hpf), during the time of motor nerve formation[19], *nkx2.2a* RNA was restricted to the lateral floor plate (Fig. 1a,c). However, by 48 hpf, *nkx2.2a* expression was evident in cells that were outside of the ventral spinal cord, lying close to the notochord (Fig. 1e). By 72 hpf, bilateral stripes of *nkx2.2a* expression extended ventrally from the spinal cord on either side of the notochord (Fig. 1g). From a lateral view, it was apparent that peripheral *nkx2.2a* expression was segmentally iterated, similar to the pattern of motor nerves in the periphery (data not shown).

We next examined transverse sections of *Tg(nkx2.2a:megfp)* embryos, in which membrane-tethered EGFP is expressed under the control of *nkx2.2a* regulatory sequences[20,21]. Similar to *nkx2.2a* expression, at 24–36 hpf, EGFP$^+$ cells were restricted to the ventral spinal cord (Fig. 1b,d). However, at 48 and 72 hpf, EGFP$^+$ cells formed sheath-like structures in the periphery

that were continuous with the ventral spinal cord and ran ventrally down the sides of the notochord (Fig. 1f,h). Peripheral EGFP$^+$ cells often had multiple fine membrane extensions, which was suggestive of migratory activity (Fig. 1h).

The segmental distribution and sheath-like morphology of peripheral *nkx2.2a*$^+$ cells suggested that these cells wrap around motor axons. To test this hypothesis, we investigated the relationship between *nkx2.2a*$^+$ cells and motor axons that were marked by DsRed2 fluorescent protein expressed under the control of *olig2* regulatory DNA[22]. Transverse sections of *Tg (nkx2.2a:megfp);Tg(olig2:dsred2)* embryos at 48 hpf showed that EGFP$^+$ peripheral cells enveloped DsRed2$^+$ motor axons from the MEPs to the horizontal myoseptum(Fig. 2a). At 72 hpf, EGFP$^+$ cells occupied nearly the full length of the primary branches of the motor roots, but were not associated with secondary axon branches (Fig. 2b). By 96 hpf, EGFP$^+$ cells also had wrapped the secondary motor-axon branches and appeared to extend to the nerve terminals (Fig. 2c and data not shown). Distal ventral nerve roots have both motor and sensory processes. Labeling with an antibody to acetylated tubulin revealed that EGFP$^+$ cells ensheathed mixed nerves at 96 hpf, but did not extend along the sensory branch to the dorsal root ganglia (data not shown). Sections obtained from an 8-month-old *Tg(nkx2.2a:megfp)* fish revealed that motor nerve–associated EGFP$^+$ cells persisted into adulthood (Fig. 2d). These observations indicate that peripheral *nkx2.2a*$^+$ cells progressively ensheath proximal motor nerves and distal mixed motor-sensory nerves during development, forming a structure that persists for the lifetime of the animal.

We next investigated the association of *nkx2.2a*$^+$ peripheral cells with Schwann cells (Fig. 3). We crossed *Tg(nkx2.2a:megfp)* fish with *Tg(sox10(7.2):mrfp)* fish, which express membrane-tethered red fluorescence protein (RFP) in Schwann cells under the control of *sox10* regulatory DNA[20,23], to examine the spatial relationship of the two cell types. At 24 hpf, Schwann cells, but not EGFP$^+$ cells, were present at segmentally iterated positions along the trunk (Fig. 3a). By 48 hpf, however, EGFP$^+$ cells were now loosely associated with Schwann cells close to the spinal cord (Fig. 3b). By 72 hpf, EGFP$^+$ cells appeared to be tightly wrapped around Schwann cells along the motor nerves, but not around Schwann cells of the lateral line nerve (Fig. 3c). To follow up this association between *nkx2.2a*$^+$ cells and Schwann cells, we labeled *Tg (nkx2.2a:megfp)* fish with an antibody specific to myelin basic protein (MBP)[24]. This similarly revealed that EGFP$^+$ cells surround MBP$^+$ Schwann cells (Fig. 3d). Thus, peripheral *nkx2.2a*$^+$ cells ensheath both motor axons and Schwann cells.

Peripheral *nkx2.2a*$^+$ cells originate in the spinal cord

One interpretation of the data described above is that the peripheral *nkx2.2a*$^+$ cells that wrap motor axons and Schwann cells originate in the ventral spinal cord and migrate out to join the peripheral nervous system (PNS). However, an alternative interpretation of the data is that peripherally located cells, such as mesenchyme, progressively express *nkx2.2a* and wrap around motor axons and Schwann cells in a proximal to distal sequence, beginning near the MEPs. To discriminate between these possibilities, we carried out *in vivo* time-lapse imaging of *Tg(nkx2.2a:megfp)* embryos.

Beginning at approximately 45 hpf, long *nkx2.2a*$^+$ filopodia began to emerge from the ventral spinal cord at segmentally repeated positions (Fig. 4a and Supplementary Video 1 online). During the next several hours, *nkx2.2a*$^+$ cell bodies followed their processes, migrating from the spinal cord into the periphery (Fig. 4a and Supplementary Video 1). These cell bodies sometimes migrated back into the spinal cord, but always returned to the periphery where they remained (Supplementary Video 1). The *nkx2.2a*$^+$ cells often divided as they moved further into the adjacent muscle territories (Supplementary Video 2 online).

Most peripheral *nkx2.2a*$^+$ cell bodies migrated from the spinal cord by 48 hpf, approximately 30 h after the first motor axons exited. To better understand the relationship between motor axons and *nkx2.2a*$^+$ cells, we used *Tg(nkx2.2a:megfp);Tg(olig2:dsred2)* embryos for time-lapse imaging. This analysis confirmed that *nkx2.2a*$^+$ cells emerged from the spinal cord at the MEPs (Fig. 4b and Supplementary Video 3 online). Initially, EGFP$^+$ cells appeared to be broad and flat and not wrapped around motor axons. However, *nkx2.2a*$^+$ processes eventually formed sheaths that extended along and around the axons (Fig. 4b and Supplementary Video 3). These time-lapse analyses provide direct evidence that peripheral *nkx2.2a*$^+$ cells originate in the CNS, exit the spinal cord at MEPs and ensheath motor axons.

CNS-derived *nkx2.2a*$^+$ cells form the perineurium

Because *nkx2.2a*$^+$ cells that originate in the CNS wrap around both Schwann cells and axons, it seemed likely that they form the perineurium. To test this hypothesis, we assayed several defining characteristics of the perineurium, as described in other animals. First, we labeled *Tg (nkx2.2a:megfp)* fish with an antibody specific to zona occludins 1 (ZO-1), which labels tight junctions, a hallmark of the perineurium[2,4,5]. At 60 d postfertilization (dpf), EGFP fluorescence highlighted membranes that were associated with motor nerves (Fig. 5a). ZO-1 was concentrated at the same membranes, indicating the presence of tight junctions (Fig. 5a). A second feature of the perineurium is that it extends the full length of the motor nerve to the NMJ[4]. We therefore labeled *Tg(nkx2.2a:megfp)* fish with an SV2 antibody to visualize the synaptic vesicle pools concentrated at NMJs[25]. In sections of dorsal somatic muscle, SV2 labeling was always associated with EGFP$^+$ processes (Fig. 5b), indicating that peripheral *nkx2.2a*$^+$ cells extended to the NMJ. Finally, ultrastructural examination of the perineurium of rodents and birds by electron microscopy has shown concentric layers of flat cells linked by electron-dense tight junctions[6,11]. Similarly, electron microscopy studies of zebrafish showed that motor nerves were surrounded by concentric layers of flat cells, and that these cells were linked by characteristic electron-dense tight junctions (Fig. 5c,d). Each cell layer was associated with basal lamina on both sides, another characteristic feature of perineurial cells (Fig. 5d). On the basis of these criteria, we conclude that the zebrafish perineurium is structurally similar to the perineurium of other vertebrate species and arises from *nkx2.2a*$^+$ cells that migrate from the CNS, instead of arising from mesenchymal cells in the vicinity of motor nerves. Hereafter, we will refer to these cells as perineurial glia to reflect their neural origin.

Absence of perineurial glia disrupts motor nerve formation

In the *Drosophila* CNS, premigratory peripheral glia are necessary for the stereotyped projection of motor axons into the periphery[17]. These cells therefore appear to act as guideposts for motor axons in the CNS. We hypothesized that the *nkx2.2a*$^+$ lateral floor-plate cells that give rise to perineurial glia similarly influence exit of pioneering neurites from the spinal cord in zebrafish. Previous work established that *nkx2.2a* is required for lateral floor-plate development in zebrafish[18].We therefore interfered with *nkx2.2a*function using antisense morpholino oligonucleotides, and assayed the consequences on motor projections.

To test the efficacy of *nkx2.2a* morpholino oligonucleotides, we first assessed expression of genes that mark ventral spinal-cord cells. In wild-type embryos, *foxa2* expression marks both medial and lateral floor-plate cells[26] (Supplementary Fig. 1 online). In morpholino oligonucleotide–injected embryos, *foxa2* expression was reduced to a band of 1 to 2 medial floor-plate cells (Supplementary Fig. 1). *nkx2.2b* expression normally marks lateral floor plate and interspersed V3 interneurons, but in the absence of *nkx2.2a* function, *nkx2.2b* was only expressed in presumptive V3 interneurons[18]. Consistent with this, fewer ventral spinal-cord cells expressed *nkx2.2b* in *nkx2.2a* morpholino oligonucleotide–injected embryos compared

with controls (Supplementary Fig. 1). Thus, *nkx2.2a* morpholino oligonucleotide injections effectively reduce gene expression that marks the lateral floor plate.

We designed *nkx2.2a* MO1 (morpholino oligonucleotide 1) to block translation of the endogenous *nkx2.2a* gene, but not translation of *egfp* mRNA expressed by the transgene (Methods). This allowed us to use EGFP fluorescence as a marker of cells that expressed *nkx2.2a* in MO1-injected embryos (Fig. 6). We injected *nkx2.2a* MO1 into *Tg (nkx2.2a:megfp);Tg(olig2:dsred2)* embryos. Similar to wild-type embryos, ventral spinal-cord cells of injected embryos expressed high levels of EGFP (Fig. 6a–f). However, EGFP$^+$ cells failed to migrate from the ventral spinal cord (Fig. 6d,f and Supplementary Table 1 online). Although motor axons of MO1-injected larvae were associated with NMJs, perineurial cell tight junctions were absent (Supplementary Fig. 2 online). Taken together with data showing that *nkx2.2a* is necessary for expression of genes that mark lateral floor plate[18] (Supplementary Fig. 1) and that *nkx2.2a*$^+$ lateral floor-plate cells give rise to perineurial glia (Fig. 1–Fig. 5), these results show that formation of the perineurium requires *nkx2.2a* function.

In control embryos, motor nerve projections were highly regular and tightly fasciculated (Fig. 6a,b and Supplementary Tables 1 and 2 online). In contrast, many motor axons in all morpholino oligonucleotide–injected embryos exited the spinal cord at irregular positions, causing a severe disruption of the normal segmental distribution (Fig. 6d,i and Supplementary Table 2). The motor axons in morpholino oligonucleotide–injected embryos were often stunted relative to control embryos, and the nerves appeared thinner and had more branches, suggesting that the motor axons did not form tight fascicles (Fig. 6a–f,j and Supplementary Tables 1 and 2). Additionally, a subset of morpholino oligonucleotide–injected embryos had DsRed2$^+$ cell bodies outside of the spinal cord, showing that, in the absence of lateral floor plate and perineurial glia, motor neuron soma followed their axons into the periphery (Fig. 6e,f and Supplementary Table 1). These data indicate that *nkx2.2a*$^+$ cells are necessary for exit of bundled motor axons at regular positions in the ventral spinal cord and to prevent motor neuron migration from the CNS.

As an independent method to eliminate lateral floor plate and perineurial glia, we interfered with Hedgehog (Hh) signaling. Zebrafish embryos homozygous for mutations of *sonic hedgehog a (shha)*, which encodes one of five known Hh proteins, lack lateral floor plate, but have motor neurons[27]. Consequently, we speculated that low concentrations of cyclopamine, a pharmacological inhibitor of the Hh signaling pathway[28,29], could similarly block lateral floor-plate formation with-out disrupting motor neuron development. We first determined that treatment with 25 μM cyclopamine at 9–10 hpf abolished *nkx2.2a* expression (Supplementary Fig. 3 online), but did not affect motor neuron number (n = 30 embryos) (Fig. 6g,h). We next exposed *Tg(olig2:dsred2)* embryos to 25 μM cyclopamine at 9 hpf (n = 60 embryos). Similar to *nkx2.2a* morpholino oligonucleotide–injected embryos, motor axons exited the spinal cord at irregular positions and appeared to be poorly fasciculated (Fig. 6g–j and Supplementary Table 2). Thus, two independent, but complementary, approaches support the conclusion that *nkx2.2a*$^+$ lateral floor-plate cells and their descendent perineurial glia guide motor axon exit from the CNS and facilitate axonal fasciculation.

To investigate the effect of the absence of perineurial glia on Schwann cell development, we injected *Tg(nkx2.2a:megfp);Tg(sox10(7.2):mrfp)* embryos with *nkx2.2a* morpholino oligonucleotides. At 24 hpf, Schwann cells in morpholino oligonucleotide–injected embryos remained close to the ventral spinal cord, instead of extending along motor axons as they do during the normal developmental progression (Fig. 7a,b). By 48 hpf, Schwann cells in wild-type embryos had begun to form contiguous sheaths around motor axons (Fig. 7c). In contrast, Schwann cells in morpholino oligonucleotide–injected embryos appeared to be isolated, as individual, irregularly shaped cells at ectopic positions (Fig. 7d and Supplementary Table 1).

Consistent with this, MBP was absent from motor nerves in morpholino oligonucleotide–injected larvae (Supplementary Fig. 2). Thus, in the absence of perineurial glia, Schwann cells failed to wrap around and myelinate motor nerves normally.

Perineurial glia differentiation depends on Schwann cells

Previous studies demonstrated that Schwann cell–derived Dhh is necessary for development of the perineurial sheath, leading to the proposal that Dhh promotes a mesenchymal-to-epithelial transformation of nearby fibroblasts[12]. However, the above data provide compelling evidence that the perineurium forms from glial cells that migrate out of the ventral spinal cord, changing this interpretation. To investigate whether perineurial glia differentiation requires signals from Schwann cells, we examined *colorless (cls)* mutant fish[30], which are deficient for Sox10, a transcription factor that is necessary for Schwann cell development[31–33].

To image Schwann cells in the absence of Sox10, we produced *cls* mutant embryos carrying the *Tg(sox10(7.2):mrfp)* transgene. *sox10*$^{+}$ cells were present in mutant embryos, but their morphologies were markedly different from wild type (Supplementary Fig. 4 online). Specifically, *sox10*$^{+}$ cells often appeared as individuals, rather than as contiguous columns of cells associated with the motor nerves, and many did not wrap around axons. Thus, in the absence of Sox10 function, Schwann cells failed to coordinately wrap around motor nerves.

Next, we created *Tg(nkx2.2a:megfp)* embryos homozygous for two different *cls* alleles, *cls*^{m241} and *cls*^{tw11} (Fig. 8). Time-lapse imaging in wild-type embryos showed that perineurial glia extend into the periphery as contiguous sheaths around motor nerves (Supplementary Video 3). In contrast, *nkx2.2a*$^{+}$ cells in *cls* mutant embryos migrated away from the ventral spinal cord as individuals and never wrapped around motor nerves (Fig. 8a,b and Supplementary Videos 4 and 5 online). In mutant embryos, *nkx2.2a*$^{+}$ cells had abnormally long and excessively active filopodia, suggesting that signals from Schwann cells are necessary to appropriately guide migration (Fig. 8a,b and Supplementary Videos 4 and 5). Thus, we conclude that Schwann cell differentiation is necessary for the coordinated migration and motor nerve–ensheathing activities of perineurial glia.

Finally, we asked whether the failure of perineurial cell differentiation in *sox10* mutant embryos affects motor nerve formation. We labeled *cls* mutant embryos with antibody to znp-1, which labels primary motor axons, the first motor axons to project from the spinal cord[19]. By 48 hpf, primary motor axons in both *cls*^{m241} and *cls*^{tw11} mutant embryos exited the spinal cord, but were more highly branched than those in wild type, suggesting that they were poorly fasciculated (Fig. 8c–e,g and Supplementary Table 2). However, in contrast to *nkx2.2a* morpholino oligonucleotide–injected embryos, all motor axons projected from the spinal cord at their normal, segmental positions (Fig. 8c–f and Supplementary Table 2). We interpret this to mean that, in *cls* mutant embryos, perineurial glia can act at MEPs to help guide motor axon exit, but that the subsequent failure of motor nerve wrapping by Schwann cells and perineurial glia permits abnormal motor axon branching.

DISCUSSION

Perineurial glia origins

The CNS is shielded from infection, mechanical insults and depolarizing ionic conditions by the meninges, a system of membranes composed of dura mater, arachnoid mater and pia mater. Pia mater, the innermost layer that directly contacts neurons, consists of multiple layers of flat, squamous epithelial cells. Peripheral nerves are similarly enclosed by the flattened cells of the perineurium. The pia mater is continuous with the perineurium at the interfaces of the CNS and PNS, and together they serve to safely partition the nervous system from the rest of the

body. The origins and developmental roles of these ensheathing cells have received considerably less attention than the neurons and associated myelinating glia that they protect. Consequently, a question as simple as, "Where do perineurial cells come from?" has remained unanswered since they were reported more than 150 years ago.

One possibility is that perineurial cells arise from mesoderm. Perineurial cells have been described as mesenchyme or fibroblasts because, similar to fibroblasts, they have collagen fibers[4,11,34] and it seemed that the perineurium was organized during development from cells that were loosely associated with nerves[11,12]. In support of this idea, fibroblasts cultured in the presence of neurons and Schwann cells form perineurial-like structures[35]. However, other characteristics, such as association of perineurial cells with basal lamina, are quite different from fibroblasts[4]. Another possibility is that perineurial cells arise from neural crest. However, in culture, neural crest–derived Schwann cells do not form perineurium[35] and *in vivo* cell-lineage experiments have shown that neural crest contributes to nerve-associated endoneurium, but not to perineurium[36]. A third possible source of perineurial cells is the CNS. Examination of neural crest–ablated chick embryos and xenografted amphibian embryos revealed an apparent contribution of neural tube cells to ventral nerves[37,38]. Similarly, labeled chick neural-tube grafts gave rise to cells that were associated with ventral nerves that were described as Schwann sheath cells[39]. However, the identities of neural tube–derived cells in these experiments were not determined.

More recent cell-labeling strategies indicate that CNS cells migrate along cranial nerves, giving rise to a large variety of derivates[40]. However, the cells were not directly observed as they underwent their implicit migrations, and the conclusions remain controversial because other investigators, after failing to achieve similar results, have suggested that problems in the cell-labeling strategies account for the apparent origin of peripheral cells in the neural tube[41,42]. The evidence for CNS-derived cells that associate with peripheral nerves is much stronger in *Drosophila*. Clonal analyses show that many peripheral glia arise from CNS neuroblasts[13], implying that peripheral glia migrate from the ventral nerve cord. Furthermore, transgenic reporter-gene expression patterns indicate that glial cells born near nerve exit and entry points migrate out of the CNS along axons and subsequently ensheath them[16]. These CNS-derived peripheral glia contribute to the blood-brain barrier[15,43] and are therefore functionally similar to the perineurial cells of vertebrates.

In the present study, we took advantage of the ability to directly observe cells in developing zebrafish embryos to investigate the question of perineurial cell origin. Because many neural developmental mechanisms are conserved among invertebrates and vertebrates, we reasoned that, similar to *Drosophila*, glial cells that arise close to motor neurons in the CNS might migrate out along motor axons to form the perineurium. In static images of zebrafish embryos at different stages, we observed that *nkx2.2a* is expressed first in ventral spinal cord cells and later in peripheral columns that are continuous with the neural tube. Direct evidence came from time-lapse imaging showing that *nkx2.2a*$^+$ ventral spinal cord cells emerge through the MEPs, wrap around both motor axons and Schwann cells and extend as sheaths to the motor nerve terminals. The ensheathing *nkx2.2a*$^+$ cells form numerous tight junctions and do not express MBP, indicating that they form the perineurium. Thus, our work provides evidence that motor nerve–associated perineurial cells originate in the CNS. Because these peripheral cells arise from ventral spinal cord, mutations that alter neural tube dorsoventral patterning may have previously unanticipated consequences for PNS development.

Perineurial glia functions

A notable feature of embryos without perineurial glia is the fact that motor axons exit the spinal cord at ectopic positions. Moreover, these axons are abnormally branched and have defasciculated trajectories. To our surprise, motor-neuron cell bodies often escape the spinal

cord, a phenotype previously associated with reduced levels of Hh signaling[44]. These observations raise the possibility that perineurial glia have two distinct functions before migration. First, the ectopic motor-axon exit implies that, similar to CNS glia of flies[17], zebrafish perineurial glia help determine the position of MEPs. Second, the aberrant migration of motor neuron soma from the spinal cord suggests that perineurial glia contribute to the interface between the CNS and PNS. Neural crest–derived boundary cap cells, which transiently assemble at MEPs on the outside of the spinal cord, have a similar role in confining motor-neuron cell bodies to the neural tube in rodents and birds[1]. Future experiments will need to address whether this function of perineurial glia is unique to zebrafish or if perineurial glia and boundary cap cells coordinately act at MEPs in all vertebrates.

After migration into the periphery, perineurial glia direct the formation of tightly fasciculated, myelinated motor nerves. In the absence of perineurial glia, Schwann cells fail to target and wrap around motor axons. This could be an indirect consequence of ectopic axon exit. However, many axons still project from their normal positions in *nkx2.2a* morpholino oligonucleotide–injected embryos, raising the possibility that cues derived from perineurial glia attract Schwann cells or promote their differentiation. Conversely, Schwann cells also direct perineurial cell behavior. In *cls/sox10* mutant embryos, in which Schwann cells do not differentiate, *nkx2.2a*$^{+}$ cells migrate from the spinal cord, but do not wrap around motor nerves, implying the action of a Schwann cell–to–perineurial cell signal. In fact, one such signal has already been identified. Mouse Schwann cells express Dhh, and in its absence perineurial cells fail to create tight barriers around motor nerves. These findings led to the proposal that Dhh causes nearby fibroblasts to undergo a mesenchymal-to-epithelial transition and form the perineurium[12]. Our work suggests that reciprocal signaling between two classes of glia coordinates their differentiation and orchestrates development of fully myelinated and ensheathed motor nerves.

In summary, our work shows that the perineurium develops from glial cells that originate in the CNS and that these are actively involved in the formation of motor nerve roots through interactions with motor axons and Schwann cells. Our data should prompt a reexamination of the identity and origin of perineurial cells in mammals and further investigation of the molecules that promote their differentiation. Defects in perineurial glia might contribute to diseases disrupting nerve root development or maintenance. For example, Charcot-Marie-Tooth disease, which comprises a group of peripheral neuropathies, often results from defects of axons or Schwann cells, but the primary defects underlying some Charcot-Marie-Tooth disease variants are not well understood[45–47]. Additionally, many peripheral nerve–sheath tumors are described as perineurial[48,49], raising the possibility that defects in perineurial glia proliferation contribute to cancer. A more complete understanding of the role of perineurial glia in neural development should help to bring new insights into these diseases of the peripheral nervous system.

METHODS

Fish husbandry

All animal studies were approved by the Vanderbilt University Institutional Animal Care and Use Committee. Zebrafish strains used in this study included AB, *Tg(nkx2.2a:megfp)*^{vu17} (ref. 20), *Tg(olig2:dsred2)*^{vu19}, *Tg(sox10 (7.2):mrfp)*^{vu234}, *cls*^{tw11} (refs. 30,50) and *cls*^{m241}. Embryos were produced by pair-wise matings, raised at 28.5 °C in egg water or embryo medium and staged according to hpf or dpf. Embryos used for *in situ* hybridization, immunocytochemistry and microscopy were treated with 0.003% phenylthiourea in egg water to reduce pigmentation.

In vivo imaging

At 24 hpf, all embryos used for live imaging were manually dechorionated and transferred to egg water containing phenylthiourea. At specified stages, embryos were anesthetized using 3-aminobenzoic acid ethyl ester (Tricaine), immersed in 0.8% low–melting temperature agarose and mounted on their sides in glass-bottomed 35-mm Petri dishes (World Precision Instruments). All images were captured using a 40× oil-immersion (NA = 1.3) objective mounted on a motorized Zeiss Axiovert 200 microscope equipped with a PerkinElmer ERS spinning-disk confocal system. During time-lapse experiments, a heated stage chamber was used to maintain embryos at 28.5 °C. *Z* image stacks were collected every 5–10 min, and three-dimensional datasets were compiled using Sorenson 3 video compression (Sorenson Media) and exported to QuickTime (Apple) to create movies.

In situ hybridization

Embryos and larvae were fixed in 4% paraformaldehyde for 24 h, stored in 100% methanol at −20 °C and processed for *in situ* RNA hybridization. Plasmids were linearized with appropriate restriction enzymes and cRNA preparation was carried out using Roche DIG-labeling reagents and T3, T7 or SP6 RNA polymerases (NEB). After the *in situ* hybridization, embryos were embedded in 1.5% agarose/30% sucrose and frozen in 2-methyl butane chilled by immersion in liquid nitrogen. We collected 10-μm transverse sections on microscope slides using a cryostat microtome and covered with 75% glycerol. Images were obtained using a Retiga Exi–cooled CCD camera (Qimaging) mounted on an Olympus AX70 microscope equipped with Openlab software (Improvision). All images were imported into Adobe Photoshop. Adjustments were limited to levels, contrast, color matching settings and cropping.

Immunocytochemistry

Embryos and larvae were fixed in AB Fix (4% paraformaldehyde, 8% sucrose, 1× PBS) for 3 h at 23 °C or overnight at 4 °C and embedded as described above. We collected 10–50-μm transverse sections using a cryostat microtome. Sections were rehydrated in 1× PBS for 60 min at 23 °C and preblocked in 2% sheep serum/BSA–1× PBS for 30 min. Sections were incubated with primary antibody overnight at 4 °C. The primary antibodies used included mouse antibody to ZO-1 (Zymed, 1:200), mouse antibody to SV2 (Developmental Studies Hybridoma Bank, 1:500) and rabbit antibody to MBP[24] (gift from Will Talbot, Stanford University, 1:1,000). Sections were washed extensively with 1× PBS, incubated for 3 h at 23 °C with either Alexa Fluor 568 goat antibody to rabbit or Alexa Fluor 568 goat antibody to mouse (Molecular Probes) as secondary antibodies for detection of primary antibodies, and washed with 1× PBS for 30 min. Sections were mounted in Vectashield (Vector Laboratories) and imaged using the confocal microscope described above. Image adjustments were limited to contrast enhancement and levels settings using Volocity software (Improvision) and Adobe Photoshop.

Electron microscopy

60-dpf adults were euthanized with Tricaine and the trunk was cut into thin sections (2–3 mm in width) to allow for good penetration of fixative. Samples were fixed in 2% glutaraldehyde in 0.05 M PBS for 1 h and placed into fresh 2% glutaraldehyde overnight. Samples were washed in PBS for 30 min, transferred to 1% O_sO_4 in PBS with 1.5% $K_3Fe(CN)_63H_2O$[276] for 3 h and washed three times in dH_2O. Preparations were stained *en bloc* in 1% aqueous uranyl acetate for 1 h and washed three times in dH_2O. Samples were then subjected to ethanol dehydration: 30% ethanol for 10 min twice, 50% ethanol for 10 min twice, 50% ethanol for 15 min twice, 70% ethanol for 30 min twice, 100% ethanol for 20 min three times and 100% ethanol for 60 min twice, and passed through two 20-min incubations with propylene oxide as a transition. Preparations were transferred to a 1:1 araldite:propylene-oxide mixture for 1 h and 1:3 araldite:propyleneoxide for 3 h, which was followed by complete infiltration of pure araldite

facilitated with the help of a vacuum oven for 1 h. Samples were placed into fresh araldite and left to cure overnight in a 60 °C oven. Ultra-thin sections (60–70 nm) were obtained on a Leica UCT Ultracut microtome, transferred to formvar-coated grids and examined on a Phillips CM10 TEM equipped with an AMT 2 mega-pixel camera.

Cyclopamine treatment

Embryos were incubated beginning at 9 hpf in embryo medium containing 25 μM cyclopamine (Toronto Research Chemicals), diluted from a 10 mM stock in ethanol, at 28.5 °C. To stop the treatment, embryos were rinsed three times in fresh embryo medium.

Morpholino injections

Morpholino antisense oligonucleotides were purchased from Gene Tools. *nkx2.2a* MO1 (5′-CCG TCT TTG TGT TGG TCA ACG ACA T-3′) was complementary to a sequence spanning just before and including the translation start codon[18]. *nkx2.2a* MO2 (5′-AAG TTG CTG CAC CAG TTT GAC AAT C -3′) was complementary to a sequence in the 5′ UTR. Morpholino oligonucleotides were dissolved in water to create a stock solution of 3 mM and diluted in 2× injection buffer (5 mg ml^{-1} Phenol red, 40 mM HEPES and 240 mM KCl) to create a working injection concentration of 0.5 mM for MO1 and 0.75 mM for MO2. We injected 2–4 nl into the yolk just below the single cell of fertilized embryos. All morpholino oligonucleotide injected embryos were raised in embryo medium at 28.5 °C.

Quantification of motor axon phenotype and statistical analysis

To measure motor nerve–root periodicity in morpholino oligonucleotide–injected and wild-type embryos, composite *Z* image stacks were compiled using Volocity software. The distance between each motor nerve root was determined by drawing a line from the center of each exiting motor nerve to the next. Root periodicity was determined between somites 8 and 12. The number of axon branches to the horizontal myoseptum was determined by following axon bundles using the XYZ function of Volocity. Individual *Z* images were sequentially observed and branches counted. For morpholino oligonucleotide–injected embryos in which the horizontal myoseptum was not clear, axon branches were counted over a distance of 52 μm from the spinal cord, which is the average distance to the horizontal myoseptum in control embryos. Axon branching was also determined between somites 8 and 12. All graphically presented data represents the mean of the analyzed data. Statistical analyses were performed with Prism software. The level of significance was determined by either paired or unpaired *t*-tests using a confidence interval of 95%.

Supplementary Material

Refer to Web version on PubMed Central for supplementary material.

ACKNOWLEDGMENTS

We thank T. Piotrowski, J. Shin, W. Talbot and R. Karlstrom for reagents and fish, M. Bhat, V. Auld and members of the Appel lab for valuable discussions, and J. Weston for comments on the manuscript. Reagents also were provided by the Zebrafish International Resource Center, supported by grant P40 RR012546 from the US National Institutes of Health (NIH) National Center for Research Resources. This work was supported by the Post Doctoral Training Program in Neurogenomics-MH65215-03 (S.K.), NIH grant R01 NS046668 (B.A.), NIH grant R01 GM054544 (K.B.) and a zebrafish initiative funded by the Vanderbilt University Academic Venture Capital Fund.

References

1. Vermeren M, et al. Integrity of developing spinal motor columns is regulated by neural crest derivatives at motor exit points. Neuron 2003;37:403–415. [PubMed: 12575949]

2. Akert K, Sandri C, Weibel ER, Peper K, Moor H. The fine structure of the perineural endothelium. Cell Tissue Res 1976;165:281–295. [PubMed: 1082372]

3. Allt G. Ultrastructural features of the immature peripheral nerve. J. Anat 1969;105:283–293. [PubMed: 5809407]

4. Bourne, GH. The Structure and Function of Nervous Tissue. Vol. Vol. V. New York: Academic Press; 1968.

5. Burkel WE. The histological fine structure of perineurium. Anat. Rec 1967;158:177–189. [PubMed: 6039587]

6. Haller FR, Low FN. The fine structure of the peripheral nerve root sheath in the subarachnoid space in the rat and other laboratory animals. Am. J. Anat 1971;131:1–19. [PubMed: 5089840]

7. Nordlander RH, Singer JF, Beck R, Singer M. An ultrastructural examination of early ventral root formation in amphibia. J. Comp. Neurol 1981;199:535–551. [PubMed: 7276239]

8. Guyton, AC. Structure and Function of the Nervous System. Philadelphia: Saunders; 1972. Ch. 14; p. 254

9. Kristensson K, Olsson Y. The perineurium as a diffusion barrier to protein tracers. Differences between mature and immature animals. Acta Neuropathol. (Berl.) 1971;17:127–138. [PubMed: 5101596]

10. Olsson Y. Microenvironment of the peripheral nervous system under normal and pathological conditions. Crit. Rev. Neurobiol 1990;5:265–311. [PubMed: 2168810]

11. Du Plessis DG, Mouton YM, Muller CJ, Geiger DH. An ultrastructural study of the development of the chicken perineurial sheath. J. Anat 1996;189:631–641. [PubMed: 8982839]

12. Parmantier E, et al. Schwann cell–derived Desert hedgehog controls the development of peripheral nerve sheaths. Neuron 1999;23:713–724. [PubMed: 10482238]

13. Schmidt H, et al. The embryonic central nervous system lineages of *Drosophila melanogaster*. II. Neuroblast lineages derived from the dorsal part of the neuroectoderm. Dev. Biol 1997;189:186–204. [PubMed: 9299113]

14. Klambt C, Goodman CS. The diversity and pattern of glia during axon pathway formation in the *Drosophila* embryo. Glia 1991;4:205–213. [PubMed: 1827779]

15. Parker RJ, Auld VJ. Roles of glia in the *Drosophila* nervous system. Semin. Cell Dev. Biol 2006;17:66–77. [PubMed: 16420983]

16. Sepp KJ, Schulte J, Auld VJ. Developmental dynamics of peripheral glia in *Drosophila melanogaster*. Glia 2000;30:122–133. [PubMed: 10719354]

17. Sepp KJ, Schulte J, Auld VJ. Peripheral glia direct axon guidance across the CNS/PNS transition zone. Dev. Biol 2001;238:47–63. [PubMed: 11783993]

18. Schafer M, Kinzel D, Winkler C. Discontinuous organization and specification of the lateral floor plate in zebrafish. Dev. Biol 2007;301:117–129. [PubMed: 17045256]

19. Myers PZ, Eisen JS, Westerfield M. Development and axonal outgrowth of identified motoneurons in the zebrafish. J. Neurosci 1986;6:2278–2289. [PubMed: 3746410]

20. Kirby BB, et al. *In vivo* time-lapse imaging shows dynamic oligodendrocyte progenitor behavior during zebrafish development. Nat. Neurosci 2006;9:1506–1511. [PubMed: 17099706]

21. Ng AN, et al. Formation of the digestive system in zebrafish. III. Intestinal epithelium morphogenesis. Dev. Biol 2005;286:114–135. [PubMed: 16125164]

22. Shin J, Park HC, Topczewska JM, Mawdsley DJ, Appel B. Neural cell fate analysis in zebrafish using olig2 BAC transgenics. Methods Cell Sci 2003;25:7–14. [PubMed: 14739582]

23. Carney TJ, et al. A direct role for Sox10 in specification of neural crest–derived sensory neurons. Development 2006;133:4619–4630. [PubMed: 17065232]

24. Lyons DA, et al. erbb3 and erbb2 are essential for schwann cell migration and myelination in zebrafish. Curr. Biol 2005;15:513–524. [PubMed: 15797019]

25. Ono F, Mandel G, Brehm P. Acetylcholine receptors direct rapsyn clusters to the neuromuscular synapse in zebrafish. J. Neurosci 2004;24:5475–5481. [PubMed: 15201319]

26. Odenthal J, Nusslein-Volhard C. Fork head domain genes in zebrafish. Dev. Genes Evol 1998;208:245–258. [PubMed: 9683740]

27. Schauerte HE, et al. Sonic hedgehog is not required for the induction of medial floor plate cells in the zebrafish. Development 1998;125:2983–2993. [PubMed: 9655820]

28. Incardona JP, Gaffield W, Kapur RP, Roelink H. The teratogenic Veratrumalkaloid cyclopamine inhibits sonic hedgehog signal transduction. Development 1998;125:3553–3562. [PubMed: 9716521]
29. Cooper MK, Porter JA, Young KE, Beachy PA. Teratogen-mediated inhibition of target tissue response to Shh signaling. Science 1998;280:1603–1607. [PubMed: 9616123]
30. Dutton KA, et al. Zebrafish colourless encodes sox10 and specifies non-ectomesenchymal neural crest fates. Development 2001;128:4113–4125. [PubMed: 11684650]
31. Britsch S, et al. The transcription factor Sox10 is a key regulator of peripheral glial development. Genes Dev 2001;15:66–78. [PubMed: 11156606]
32. Kuhlbrodt K, Herbarth B, Sock E, Hermans-Borgmeyer I, Wegner M. Sox10, a novel transcriptional modulator in glial cells. J. Neurosci 1998;18:237–250. [PubMed: 9412504]
33. Paratore C, Goerich DE, Suter U, Wegner M, Sommer L. Survival and glial fate acquisition of neural crest cells are regulated by an interplay between the transcription factor Sox10 and extrinsic combinatorial signaling. Development 2001;128:3949–3961. [PubMed: 11641219]
34. Gamble HJ, Eames RA. An electron microscope study of the connective tissues of human peripheral nerve. J. Anat 1964;98:655–663. [PubMed: 14229996]
35. Bunge MB, Wood PM, Tynan LB, Bates ML, Sanes JR. Perineurium originates from fibroblasts: demonstration *in vitro* with a retroviral marker. Science 1989;243:229–231. [PubMed: 2492115]
36. Joseph NM, et al. Neural crest stem cells undergo multilineage differentiation in developing peripheral nerves to generate endoneurial fibroblasts in addition to Schwann cells. Development 2004;131:5599–5612. [PubMed: 15496445]
37. Raven P. Experiments on the origin of the sheath cells and sympathetic neuroblasts in amphibia. J. Comp. Neurol 1937;67:221–240.
38. Jones DS. The origin of the sympathetic trunk in the chick embryo. Anat. Rec 1937;70:45–65.
39. Weston JA. A radioautographic analysis of the migration and localization of trunk neural crest cells in the chick. Dev. Biol 1963;6:279–310. [PubMed: 14000137]
40. Dickinson DP, Machnicki M, Ali MM, Zhang Z, Sohal GS. Ventrally emigrating neural tube (VENT) cells: a second neural tube–derived cell population. J. Anat 2004;205:79–98. [PubMed: 15291792]
41. Yaneza M, Gilthorpe JD, Lumsden A, Tucker AS. No evidence for ventrally migrating neural tube cells from the mid- and hindbrain. Dev. Dyn 2002;223:163–167. [PubMed: 11803580]
42. Boot MJ, Gittenberger-de Groot AC, van Iperen L, Poelmann RE. The myth of ventrally emigrating neural tube (VENT) cells and their contribution to the developing cardiovascular system. Anat. Embryol. (Berl.) 2003;206:327–333. [PubMed: 12649731]
43. Freeman MR, Doherty J. Glial cell biology in *Drosophila* and vertebrates. Trends Neurosci 2006;29:82–90. [PubMed: 16377000]
44. Ungos JM, Karlstrom RO, Raible DW. Hedgehog signaling is directly required for the development of zebrafish dorsal root ganglia neurons. Development 2003;130:5351–5362. [PubMed: 13129844]
45. Berger P, Niemann A, Suter U. Schwann cells and the pathogenesis of inherited motor and sensory neuropathies (Charcot-Marie-Tooth disease). Glia 2006;54:243–257. [PubMed: 16856148]
46. Meyer, Zu; Hörste, G.; Nave, KA. Animal models of inherited neuropathies. Curr. Opin. Neurol 2006;19:464–473. [PubMed: 16969156]
47. Zuchner S, Vance JM. Mechanisms of disease: a molecular genetic update on hereditary axonal neuropathies. Nat. Clin. Pract. Neurol 2006;2:45–53. [PubMed: 16932520]
48. Macarenco RS, Ellinger F, Oliveira AM. Perineurioma: a distinctive and under-recognized peripheral nerve sheath neoplasm. Arch. Pathol. Lab. Med 2007;131:625–636. [PubMed: 17425397]
49. Erlandson RA. The enigmatic perineurial cell and its participation in tumors and in tumorlike entities. Ultrastruct. Pathol 1991;15:335–351. [PubMed: 1755098]
50. Kelsh RN, et al. Zebrafish pigmentation mutations and the processes of neural crest development. Development 1996;123:369–389. [PubMed: 9007256]

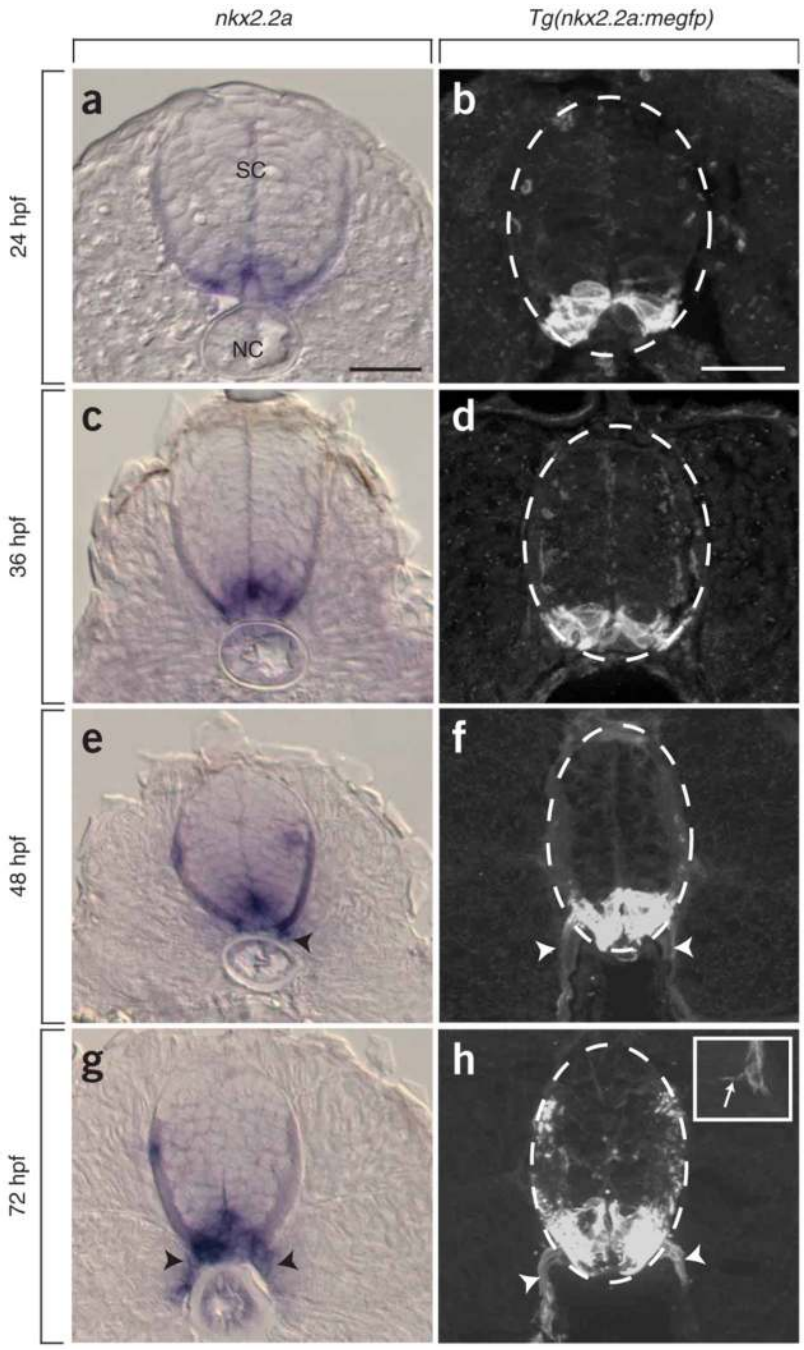

Figure 1. *nkx2.2a* expression marks peripheral cells that extend from ventral spinal cord

(**a,c,e,g**) *nkx2.2a* RNA expression was initially limited to ventral spinal cord (SC), but appeared in cells flanking notochord (NC) and was contiguous with spinal cord by 48 hpf. Arrowheads indicate *nkx2.2a*$^{+}$ cells outside of the ventral spinal cord. (**b,d,f,h**) *Tg (nkx2.2a:megfp)* EGFP expression was similar to endogenous *nkx2.2a*, appearing first in ventral spinal cord and then in sheath-like structures extending from ventral spinal cord (arrowheads). Inset (**h**) shows a higher magnification view of a filopodial process at the distal tip of a peripheral *nkx2.2a*$^{+}$ sheath. Dashed circles outline the spinal cord. All images are of 10-μm transverse sections through the trunk with dorsal to the top. Scale bars, 20 μm (**a,c,e** and **g**) and 24 μm (**b,d,f** and **h**).

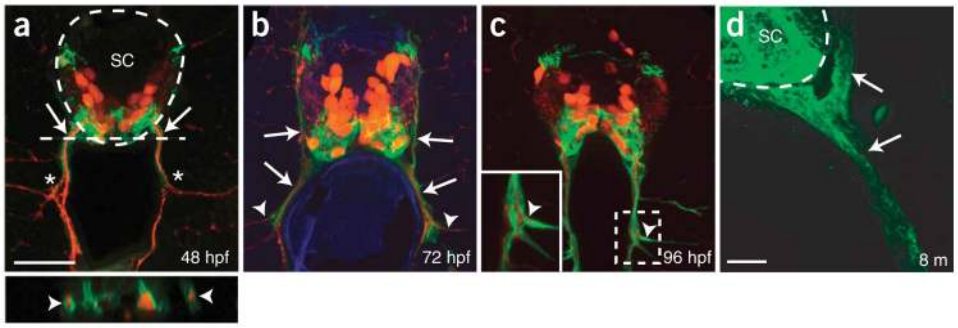

Figure 2. Peripheral *nkx2.2a*$^{+}$ cells ensheath motor axons

Transverse sections, dorsal to top, of *Tg (nkx2.2a:megfp);Tg (olig2:dsred2)* and *Tg (nkx2.2a:megfp)* animals. (**a**) At 48 hpf, EGFP^{+} cells surrounded DsRed2^{+} axons from the MEP (arrows) to the major branch point at the horizontal myoseptum (asterisks). The spinal cord (sc) is outlined. Below, orthogonal projection of the image in panel **a** at the level of the dashed line. Arrowheads point to DsRed2^{+} axons wrapped by EGFP^{+} processes. (**b**) At 72 hpf, EGFP^{+} cells ensheathed primary motor nerve branches (arrows), but not secondary axon branches (arrowheads). (**c**) At 96 hpf, EGFP^{+} cells ensheathed both primary and secondary motor-axon branches (arrowheads). Inset shows a higher magnification view of the branch point indicated by the dashed box. (**d**) EGFP expression marked the branched structure (arrows) extending from the ventral spinal cord (sc) of 8-month-old adult. Dashed line denotes the edge of the spinal cord. Scale bars, 24 μm.

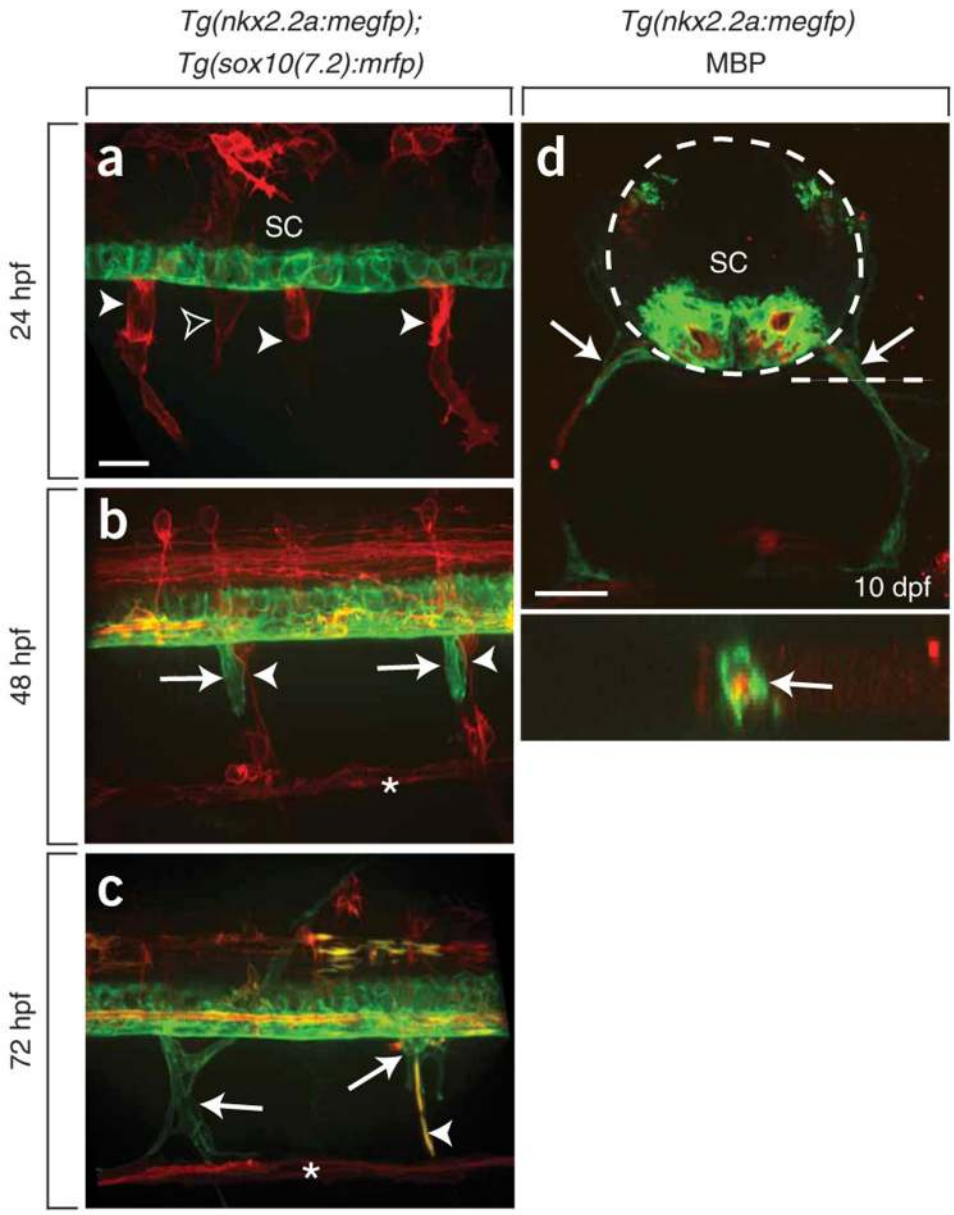

Figure 3. Peripheral *nkx2.2a*$^+$ cells ensheath Schwann cells

(**a–c**) Lateral views, with dorsal to the top, at the level of the trunk spinal cord (SC) of live *Tg (nkx2.2a:megfp);Tg(sox10(7.2):mrfp)* embryos. (**a**) By 24 hpf, RFP$^+$ Schwann cells formed segmentally iterated tubes (arrowheads). EGFP expression was limited to ventral spinal cord. Outlined arrowhead marks Schwann cell on opposite side of embryo. (**b**) By 48 hpf, peripheral EGFP$^+$ cells (arrows) appeared to emerge from the spinal cord and loosely associated with Schwann cells (arrowheads). Asterisk marks RFP$^+$ Schwann cells at the lateral line nerve. (**c**) By 72 hpf, some EGFP$^+$ cells and RFP$^+$ Schwann cells appeared to be tightly wrapped, forming slender yellow tubes (arrowhead). Other EGFP$^+$ cells remained loosely associated with the nerve (arrows). (**d**) A 10-μm transverse section of 10 dpf *Tg(nkx2.2a:megfp)* larva labeled with antibody to MBP is shown (red). EGFP$^+$ processes (arrows) surrounded MBP-labeled Schwann cells. Below, orthogonal projection at the level of dashed line. Scale bars, 24 μm (**a,b** and **c**), 12 μm (**d**) and 4 μm (orthogonal projection).

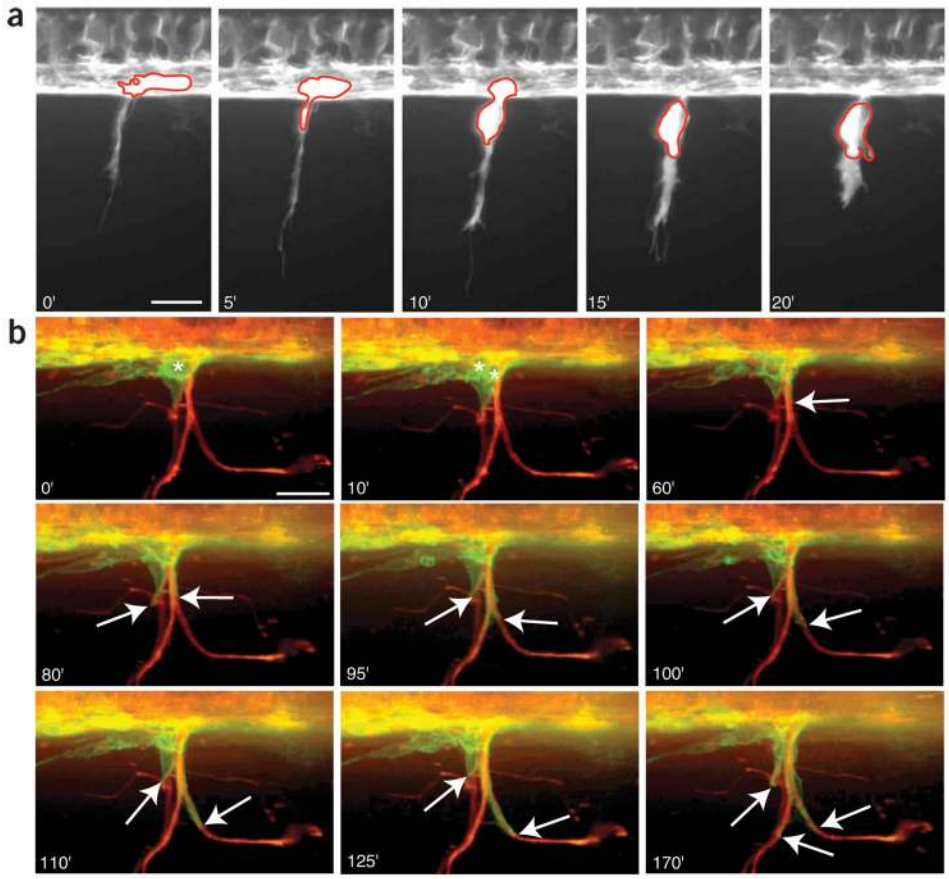

Figure 4. ***In vivo*** **time-lapse imaging reveals that peripheral** ***nkx2.2a***$^{+}$ **cells originate in the CNS and ensheath ventral motor-nerve roots**

(**a**) Frames captured from a 24-h time-lapse sequence (Supplementary Video 1) of a *Tg (nkx2.2a:megfp)* embryo beginning at 40 hpf. Numbers in lower left corners denote time elapsed from the first frame. At 45 hpf (0-min time point), a long EGFP^{+} process emerged from the spinal cord, followed by the cell body, circled in red. (**b**) Frames captured from a 24-h time-lapse sequence (Supplementary Video 3) of a *Tg(nkx2.2a:megfp);Tg(olig2:dsred2)* embryo, beginning at 52 hpf. At 56 hpf (0-min time point), an EGFP^{+} cell (asterisk) had emerged from the spinal cord and had begun to extend along the DsRed2^{+} motor nerve. The cell divided (asterisks) and both cells began to extend as sheath-like structures along motor axons (arrows) 10 min later. All images are lateral views at the level of the trunk spinal cord with dorsal to the top and anterior to the left. Scale bars, 12 μm.

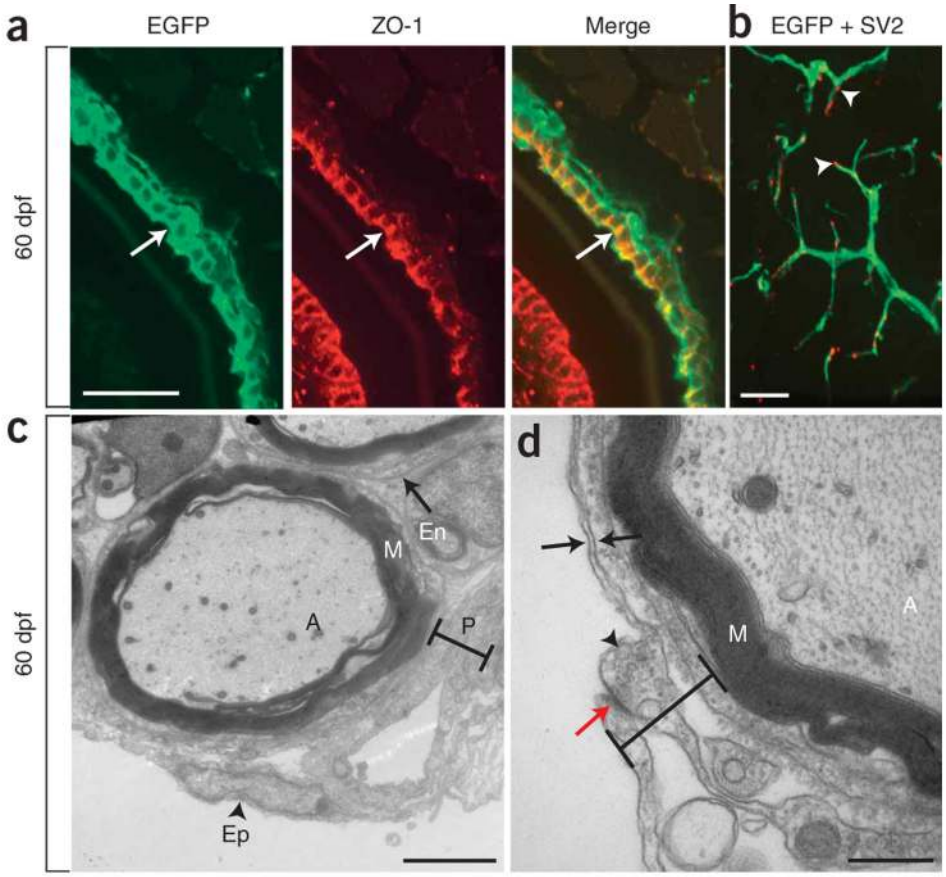

Figure 5. Peripheral *nkx2.2a*$^{+}$ cells form the perineurium

(**a**) Transverse section of a 60-dpf *Tg(nkx2.2a:megfp)* animal. Antibody to ZO-1 labeled EGFP^{+} membranes at the motor nerve (arrows). (**b**) In dorsal somatic muscle, SV2^{+} NMJs (red) concentrated along the tips of EGFP^{+} processes (arrowheads). (**c**) Electron micrograph of a motor nerve in a 60-dpf animal. Perineurial (P) cell processes (cross bar) surrounded axons (A) that were wrapped by myelinating Schwann cells (M). En, endoneurium; Ep, epineurium. (**d**) Higher magnification view of a motor nerve. Perineurial cells were associated with basal lamina (black arrow), tight junctions (red arrow) and pinocytotic vesicles (arrowhead). Cross bar demarcates perineurium. Scale bars, 24 μm (**a,b**) and 500 nm (**c,d**).

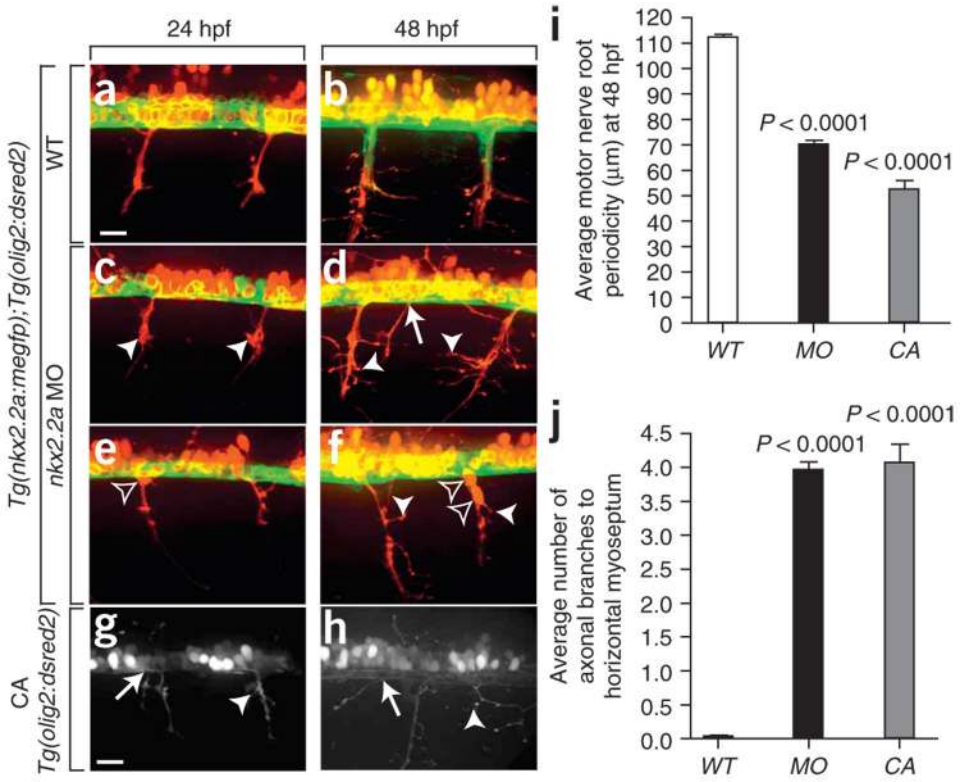

Figure 6. Absence of perineurial glia causes aberrant motor-axon projection

(**a–f**) Comparison of perineurial cell migration and axon projection in wild-type (WT) and *nkx2.2a* morpholino oligonucleotide–injected embryos. Although ventral spinal-cord cells of morpholino oligonucleotide–injected embryos expressed EGFP, perineurial glia did not migrate from the spinal cord. Axons projected from the spinal cord at irregular, ectopic positions (arrows) and appeared defasciculated (arrowheads). (**e,f**) *olig2*$^{+}$ cell bodies were often located outside of the spinal cord (outlined arrowheads) in morpholino oligonucleotide–injected embryos. (**g,h**) Motor axons exited the spinal cord at ectopic positions (arrows) and appeared defasciculated (arrowheads) in cyclopamine-treated embryos. (**i**) Quantification of the motor axon exit defect by measurement of the distance between motor nerve roots. Morpholino oligonucleotide–injected and cyclopamine-treated embryos had significantly shorter distances between motor roots compared with WT. (**j**) Quantification of motor nerve defasciculation by determination of the number of axon branches between the spinal cord and horizontal myoseptum. Morpholino oligonucleotide–injected and cyclopamine-treated embryos had significantly more branches than WT embryos. Statistical significance was determined using the unpaired *t*-test. *P* values are shown for each experimental condition compared with WT. All images are lateral views at the level of the trunk spinal cord of living embryos with dorsal to the top and anterior to the left. Scale bar, 24 μm.

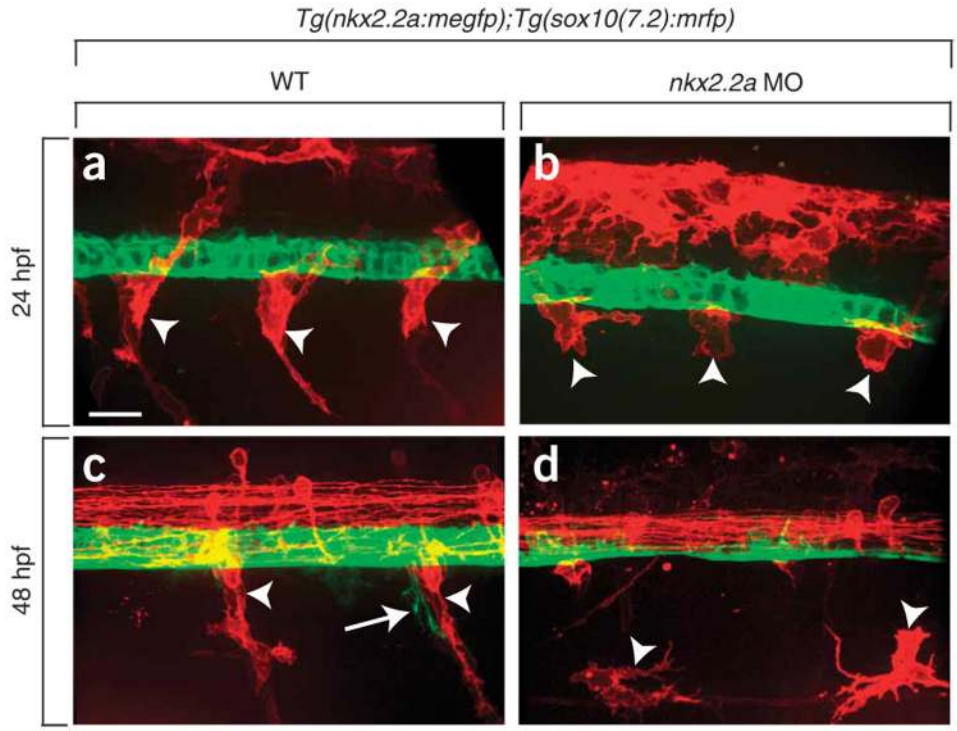

Figure 7. Removal of *nkx2.2a* function perturbs Schwann cell development

(**a,b**) By 24 hpf, Schwann cells (arrowheads) migrated to ventral spinal cord of *nkx2.2a* morpholino oligonucleotide–injected embryos, but did not elongate down motor axons as they did in WT. (**c,d**) By 48 hpf, individual abnormally shaped Schwann cells migrated into the periphery of morpholino oligonucleotide–injected embryos instead of aligning with motor nerves as they did in WT (arrowheads). Arrow marks emerging perineurial glia. All images are whole mount, lateral views of live embryos with dorsal to the top and anterior to the left. Scale bar, 24 μm.

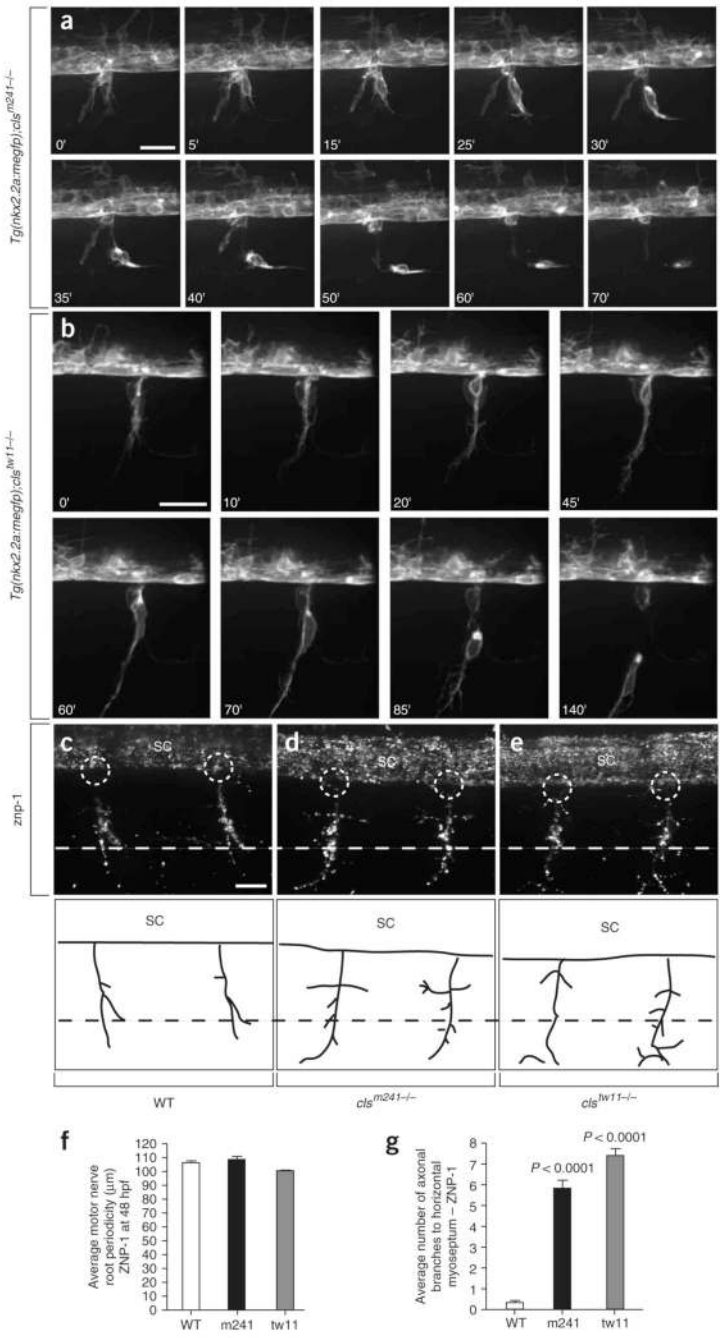

Figure 8. Schwann cell differentiation is required for ventral motor-nerve ensheathement by perineurial glia

(**a**) Frames captured from a 24-h time-lapse sequence of a *Tg(nkx2.2a:megfp);cls*$^{m241-/-}$ embryo beginning at 48 hpf (Supplementary Video 4). Numbers in lower left corners denote time elapsed from the first frame. At approximately 60 hpf (0-min time point), numerous EGFP^{+} filopodia extended from the CNS. In minutes, a cell emerged from the spinal cord (SC), dissociated from another EGFP^{+} cell and migrated away without wrapping the nerve. (**b**) Frames captured from a 24-h time-lapse sequence of a *Tg(nkx2.2a:megfp);cls*$^{tw11-/-}$ embryo beginning at 48 hpf (Supplementary Video 5). Similar to *cls*^{m241} mutants, a migrating EGFP^{+} cell failed to ensheath the nerve. (**c–e**) Znp-1 antibody labeling of primary motor axons

in 48-hpf WT, *cls*^{m241} and *cls*^{tw11} mutants. Dashed circles mark MEPs. Dashed lines mark the horizontal myoseptum. Below, tracings of znp-1–labeled motor axons in **c– e**, showing excess branches in *cls* mutants. (**f**) Quantification of the motor axon exit defect by measurement of distance between motor nerve roots. There is no difference between *cls* mutants and WT. (**g**) Quantification of motor nerve defasciculation by determination of axon branches between the spinal cord and horizontal myoseptum. *cls* mutants have significantly more branches than WT. Statistical significance was determined using the paired *t*-test. *P* values are shown for each mutant compared with WT. All images are oriented with dorsal to the top and anterior to the left. Scale bars, 12 μm (**a,b**) and 6 μm (**c–e**).